Interstitials and Vacancies in α Iron*

R. A. JOHNSON
Brookhaven National Laboratory, Upton, New York
(Received 13 January 1964)

The migration energies and atomic configurations for mono- and di-interstitials and mono- and di-vacancies in α iron have been calculated using a classical model. About 530 atoms surrounding the defect were treated as individual particles, each with three degrees of freedom, while the remainder of the crystal was treated as an elastic continuum with atoms imbedded in it. A two-body central force was devised which matched the elastic moduli, was sharply repulsive at close separation, and which went to zero midway between the second and third neighboring atoms. Configurations were found by choosing a starting configuration roughly approximating the situation under consideration and successively adjusting the value of each variable occurring in the energy equation so that the magnitude of the generalized force associated with it was zero until equilibrium was reached. The energy calculations include changes in bond energy in the discrete region, energy in the elastic field, and work done against cohesive forces, but neglect changes due to the redistribution of electrons. Calculated activation energies for motion of mono- and di-interstitials and mono- and di-vacancies were 0.33, 0.18, 0.68, and 0.66 eV, respectively, and binding energies of di-interstitials and di-vacancies were 1.08 and 0.20 eV, respectively. The stable interstitial was a "split" configuration in which two atoms were symmetrically split in a ⟨110⟩ direction about a vacant normal lattice site, and the stable di-interstitial consisted of two parallel split interstitials at nearest-neighbor lattice sites with their axes perpendicular to the line joining their centers. In the vacancy configuration an atom was missing from a normal lattice site, and the divacancy consisted of two vacancies at second-nearest-neighbor lattice sites.

INTRODUCTION

DETAILED and extensive lattice calculations for copper have been carried out for the dynamics of radiation damage events near the threshold energy for damage,[1] and for the atomic configuration[1–3] and the energy of motion[2,3] of point defects. These studies have used a similar approach to lattice calculations: The forces between atoms within a crystallite of anywhere from 50 to 1000 atoms are treated explicitly, and boundary conditions are applied to the crystallite to simulate the remainder of the lattice. The development of this method of calculation may be traced to Huntington[4] and Tewordt,[5] and a number of less extensive calculations using similar models have been performed.[6] Copper was chosen for investigation primarily because there were sufficient experimental data available, because it was felt that an appropriate and more reliable potential was available for copper than for other metals, and because the face-centered cubic structure is amenable to calculation.

The dynamic calculations[1] have recently been extended to α iron,[7] and the present research was undertaken in conjunction with that investigation. Iron was selected as the metal of greatest interest with a body-centered cubic structure. Pertinent experimental data are lacking for all body-centered cubic metals, but the threshold energy for radiation damage for α iron is known.[8]

Since the present calculation is similar to that previously used for copper by Johnson and Brown,[2] the rationale for this method will not be repeated here. In the present calculation the atoms near the defect are treated as classical particles interacting by means of a potential which applies between the first and second neighboring atoms in the lattice and which is matched to the elastic moduli.

Atomic configurations are found by choosing a starting configuration roughly approximating the situation under consideration, and then successively adjusting the value of each variable occurring in the equation for energy such that the magnitude of the generalized force associated with it is zero, and iterating this process many times. The energy in the lattice above that for a perfect lattice normally converges in the above process. Convergence is not ensured, but no difficulties have been encountered in this respect. The numerical calculations have been performed by using an IBM 7094 computer.

Iron interstitial atoms, di-interstitial pairs, vacancies, and divacancies have been studied, and the activation energy for motion as well as the atomic mechanisms of migration, as predicted by this model, have been determined for these defects. By the application of appropriate boundary conditions, the associated activation volumes for motion have also been found. Some preliminary results have been reported previously.[9]

Calculations are also being carried out for interstitial

* Work performed under the auspices of the U. S. Atomic Energy Commission.

[1] J. B. Gibson, A. N. Goland, M. Milgram, and G. H. Vineyard, Phys.Rev. **120**, 1229 (1960).

[2] R. A. Johnson and E. Brown, Phys. Rev. **127**, 446 (1962).

[3] A. Seeger, E. Mann, and R. v. Jan, Phys. Chem. Solids **23**, 639 (1962).

[4] H. B. Huntington, Phys. Rev. **91**, 1092 (1953).

[5] L. Tewordt, Phys. Rev. **109**, 61 (1958).

[6] See, for example: L. A. Girifalco and V. G. Weizer, Phys. Chem. Solids **12**, 260 (1960). K. H. Bennemann, Phys. Rev. **124**, 669 (1961). P. Hoekstra and D. R. Behrendt, Phys. Rev. **128**, 560 (1962).

[7] C. Erginsoy, G. H. Vineyard, and A. Englert, Phys. Rev. **133**, A595 (1964).

[8] P. G. Lucasson and R. M. Walker, Phys. Rev. **127**, 485 (1962).

[9] R. A. Johnson and A. C. Damask, Acta Met. **12**, 443 (1964).

impurities in α iron and these results will be reported elsewhere.

THEORY

Model

In the present calculation each atom within a spherical crystallite containing 531 atoms was treated as an independent particle. In the perfect lattice an atom was located at the center of the crystallite and the surrounding 530 atoms comprised 25 shells of symmetrically equivalent atoms.

The atoms outside the crystallite were treated as though they were imbedded in an elastic continuum. The displacement field $\mathbf{u}$ used in the present calculation for the elastic continuum is given by

$$\mathbf{u}=-C\nabla(1/r)=C(\mathbf{r}/r^3), \tag{1}$$

where C is the so-called "strength" of the displacement field. The displacement for a given atom i is given by

$$\mathbf{u}^i=C[\mathbf{r}_0{}^i/(r_0{}^i)^3],$$

where the subscript means that the term is to be evaluated at the perfect lattice position. Thus, C was used as the variable determining the displacement of all atoms outside the crystallite. Equation (1) gives rise to a spherically symmetric displacement field, for which the origin was taken as the center of the crystallite. The choice of the displacement field given by Eq. (1) is discussed in detail by Johnson and Brown.[2] This particular $\mathbf{u}$ is just one of an infinite number of solutions of the static, isotropic, elastic equation, but activation energies and atomic configurations near defects were found to be insensitive to other solutions. The effect of the displacement field given by Eq. (1) on the energies and configurations is relatively minor and this term could be eliminated from the calculation (i.e., the atoms outside the crystallite frozen at their perfect lattice positions) without introducing any serious changes in the results, but it was retained because it can be used to find activation volumes.

The energy of the crystallite is given by

$$E=\tfrac{1}{2}\sum_i\sum_j\varphi^{ij}+\sum_i\sum_k\varphi^{ik}+aC+bC^2, \tag{2}$$

where φ^{ij} is the interaction potential between atoms i and j, the i summation is over all atoms within the crystallite, the j summation is over all atoms within the crystallite which interact with the ith atom, and the k summation is over all atoms outside the crystallite which interact with the ith atom. The term aC accounts for the work done against the forces required to hold the perfect lattice in equilibrium, and the term bC^2 accounts for the energy stored within the elastic field. The energy for a particular configuration is given by $E-E_0$, where E_0 is the perfect lattice energy;

$$E_0=\tfrac{1}{2}\sum_i\sum_j\varphi_0{}^{ij}+\sum_i\sum_k\varphi_0{}^{ik}.$$

The derivation of the coefficients a and b will be given after the discussion of the potential.

The force on an atom i due to an atom j is given by

$$\mathbf{F}^{ij}=(\partial\varphi^{ij}/\partial r^{ij})(\mathbf{r}^{ij}/r^{ij}), \tag{3}$$

where $\mathbf{r}^{ij}=\mathbf{r}^j-\mathbf{r}^i$ (the vector from i to j). The total force on an atom i is then

$$\begin{aligned}\mathbf{F}^i&=-(\partial E/\partial\mathbf{r}^i)\\&=\sum_j\mathbf{F}^{ij}+\sum_k\mathbf{F}^{ik},\end{aligned} \tag{4}$$

where the summation indices have the same meaning as in Eq. (2). The generalized force on the crystallite arising for the elastic variable C is given by

$$\begin{aligned}F^c&=-(\partial E/\partial C)\\&=-\sum_i\sum_k\mathbf{F}^{ik}\cdot(\partial\mathbf{r}^k/\partial C)-a-2bC.\end{aligned} \tag{5}$$

The process for finding energy minima and saddle points was as follows: Initial vector positions of each atom within the crystallite were chosen to approximate the configuration of interest. Each coordinate of each atom within the crystallite was varied in turn until the corresponding force component became zero, and then the value of C was adjusted so that F^c was zero. Usually 10 to 20 such iterations were required for the energy and the configuration to converge sufficiently. The force on a given atom and the generalized elastic force are very nearly linear with displacement for small displacements. Thus, it was possible to find the force for a given variable at two values of the variable and use linear extrapolation to the value where the force is zero.

The volume expansion associated with a lattice configuration is easily calculated and is found to be linear with C, the elastic variable. Let $\Delta V'$ be the volume expansion of a hypothetical sphere around the defect.

$$\begin{aligned}\Delta V'&=\int\int\mathbf{u}\cdot d\mathbf{S}\\&=4\pi C.\end{aligned} \tag{6}$$

$\Delta V'$ is seen to be independent of the radius of the sphere. For a finite lattice, Eshelby[10] has shown that the boundary condition of zero stress at the surface of the lattice gives rise to an additional term in the volume expansion (the so-called "image force" correction). This correction may be written as

$$\Delta V=\Delta V'\{1+[4C_{44}{}^0/(3C_{12}{}^0+2C_{44}{}^0)]\}, \tag{7}$$

[10] J. D. Eshelby, J. Appl. Phys. 25, 255 (1954).

where the superscript indicates that the effective isotropic elastic constants, as given by Leibfried,[11] are to be used.

$$C_{12}^0=\tfrac{1}{5}(C_{11}+4C_{12}-2C_{44})$$
$$C_{44}^0=\tfrac{1}{5}(C_{11}-C_{12}+3C_{44}).$$

Applying these to Eq. (7) leads to

$$\Delta V=\Delta V'\left(1+\frac{4(C_{11}-C_{12})+12C_{44}}{15B}\right), \quad (8)$$

where B, the bulk modulus, is given by $\frac{1}{3}(C_{11}+2C_{12})$.

Potential

Experimental elastic-constant data were used as a basis for obtaining an interatomic potential for the present calculation. The elastic constants of a metal may be thought of as arising primarily from two contributions: long-range electronic interactions and short range ionic interactions. The short-range interactions predominate for transition metals, but corrections were included for the long-range terms. Analytic expressions for the electronic contribution to the elastic constants of body-centered cubic metals have been derived by Fuchs[12] using the free-electron model. Since the long-range contributions are small and since the free-electron model is expected to be a rough approximation, the calculated values were used only as a guide. The elastic moduli of iron[13] and the long- and short-range contributions used in the present calculation, in units of eV/Å^3, are listed in Table I.

The simplest type of potential that can be used in a lattice calculation is one which gives rise to central forces between pairs of atoms. The ranges of the potential must not be so large as to give rise to an interaction between distant pairs or the calculation becomes too time consuming. For the body-centered cubic lattice, it is natural to cut off the potential between the second and third nearest neighbors, since the ratio of distances to the nearest, second nearest, and third nearest neighbors is $\sqrt{3}$: 2: $2\sqrt{2}$, respectively. Thus, the first and second nearest neighbor distances are comparable, while the third nearest neighbors are considerably more distant. The body-centered cubic structure is not stable with just a nearest-neighbor central force interacting between the lattice atoms, so the potential cannot be cut off between the nearest and second nearest neighbors. Since the potential is meant to describe the short-range ionic interactions, the inclusion of only nearest and second nearest-neighbor interactions is consistent with the division of the elastic-constant data into long-range and short-range contributions.

TABLE I. Elastic moduli of iron (units of eV/Å^3).

	$C_{11}-C_{12}$	C_{44}	B
Electronic contribution	0.057	0.162	0.281
Ionic contribution	0.600	0.600	0.800
Experimental values[a]	0.657	0.762	1.081

[a] See Ref. 13.

The conditions which a spherically symmetric potential $\varphi(r)$ extending through second neighbors must fulfill to match the short-range elastic moduli are

$$(C_{11}-C_{12})_{sr}=\frac{2}{3r_2}\left(\frac{6}{r_1}\varphi_1'+3\varphi_2''+\frac{3}{r_2}\varphi_2'\right), \quad (9a)$$

$$(C_{44})_{sr}=\frac{2}{3r_2}\left(\varphi_1''+\frac{2}{r_1}\varphi_1'+\frac{3}{r_2}\varphi_2'\right), \quad (9b)$$

$$(B)_{sr}=\frac{2}{3r_2}\left(\varphi_1''-\frac{2}{r_1}\varphi_1'+\varphi_2''-\frac{2}{r_2}\varphi_2'\right), \quad (9c)$$

where the primes indicate differentiation with respect to r and the subscripts 1 or 2 mean that the term is to be evaluated at the nearest or second nearest-neighbor distance, respectively. There are three equations with four unknowns. Figure 1 indicates a family of possible curves of $\varphi'(r)$ which fit the conditions in Eq. (9) and which are zero midway between the second and third neighbor distances. The value and slope of $\varphi'(r)$ are determined at r_1 and r_2, and the value is determined at the cut off distance r_c, while the lines indicate how smooth curves might be fitted to these conditions. Curve II, which is roughly parabolic, is the "smoothest" of the family of curves, and no reason is seen to prefer any other to it. Indeed, it would be difficult to rationalize the choice of any of the other curves in preference to the parabolic one. Equation (9) contains

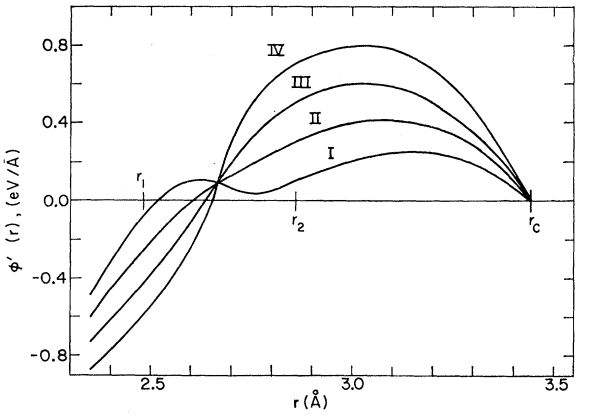

FIG. 1. A family of possible curves of the derivative of the potential, $\varphi'(r)$, which fit the short-range elastic constant conditions and which are zero midway between the second and third nearest neighbor distances.

[11] G. Leibfried, Z. Phys. **135**, 23 (1953).
[12] K. Fuchs, Proc. Roy. Soc. (London) **A153**, 622 (1936).
[13] J. A. Rayne and B. S. Chandrasekhar, Phys. Rev. **122**, 1714 (1961).

TABLE II. Iron potential.

Range (Å)	Potential (eV)
1.9–2.4	$-2.195976(r-3.097910)^3+2.704060r-7.436448$
2.4–3.0	$-0.639230(r-3.115829)^3+0.477871r-1.581570$
3.0–3.44	$-1.115035(r-3.066403)^3+0.466892r-1.547967$

three conditions and a parabola has three coefficients, so there is one parabola which fits the elastic moduli exactly. This parabola does not have a zero value midway between the second and third nearest-neighbor distances and so, another parabola was joined to it just past the second neighbor distance with matching value and slope, and zero value midway between the second and third neighbors. These parabolas represent $\varphi'(r)$, the derivative of the potential, and the actual potential was found by integration. The constant of integration was determined by the condition that the value of the potential be zero at the cutoff distance r_c.

Gibson *et al.*[1] and Erginsoy *et al.*[7] have shown that the threshold energy for radiation damage is determined primarily by the form of the potential at separations considerably less than the nearest-neighbor distance; distances which do not enter into the present calculation. It was felt, however, that the potential used here should be matched to the radiation damage potential for iron,[7] and thus, a cubic equation was joined with matching value and slope to the potential derived above at a distance just less than the nearest-neighbor distance, and was joined with matching value and slope to the dynamically determined potential at a distance less than any equilibrium distances expected from the calculation. Thus, the potential was a composite of the three cubic equations given in Table II and is shown in Fig. 2. All distances are given in Å, the iron lattice constant was taken as 2.86 Å, and energies are given in eV.

The coefficients a and b occurring in Eq. (2) may now be easily evaluated. From elastic theory, the pressure required to hold the crystallite in the perfect lattice configuration is[14]

$$P=\tfrac{1}{2}(C_{12}-C_{44})_{sr}$$
$$=\tfrac{1}{2}[(B)_{sr}-(C_{44})_{sr}-\tfrac{1}{3}(C_{11}-C_{12})_{sr}]. \quad (10)$$

For the elastic constants given in Table I for iron, $P=0$ and thus, $a=0$. The value of a may also be found by an explicit bond calculation in which Eq. (5) is evaluated for the perfect lattice with the requirement that $F^c=0$, i.e., that the perfect lattice is in equilibrium. Using the iron potential given in Table II, this calculation yields

$$a=0.0134 \text{ eV/Å}^3,$$

which value was used in the calculations. The discrepancy between this value of a and the value derived from elastic theory is negligible when compared with the magnitude of the elastic moduli. It arises because there is not an exact ratio of 4:3 of nearest to second nearest-neighbor bonds crossing the boundary between the crystallite and the elastic region.

The coefficient b was calculated from elastic theory[14] by setting the energy due to a displacement field **u** stored in the elastic field outside the crystallite equal to bC^2. This leads to

$$b=(64\pi^2/5Nr_2^3)[(C_{44})_{sr}+\tfrac{1}{3}(C_{11}-C_{12})_{sr}], \quad (11)$$

where N is the number of atoms in the crystallite. The pressure term aC plays a somewhat more important role than the elastic term bC^2, but for iron both terms could have been eliminated from the calculations with no serious effect upon the results.

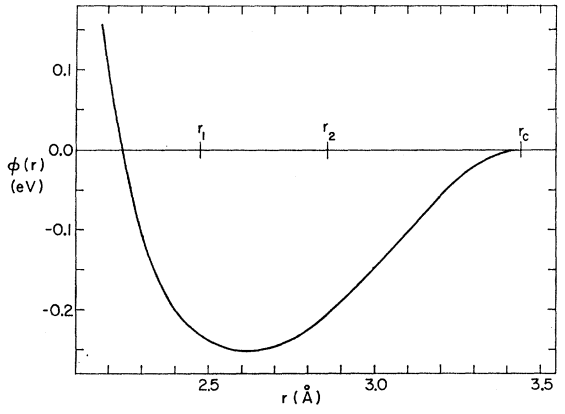

FIG. 2. The iron-iron interaction potential, $\varphi(r)$, which was used in the present calculation.

RESULTS

Interstitials

There are six interstitial configurations which must be equilibrium configurations because of symmetry, but only one of which is stable. These six configurations are denoted by the symbols I_1, $I_2 \cdots I_6$, and are described as follows: I_1 [⟨100⟩ split interstitial, Fig. 3(a)], two atoms are symmetrically split in a ⟨100⟩ direction about a vacant normal lattice site; I_2 [⟨110⟩ split interstitial, Fig. 3(b)], two atoms are symmetrically split in a ⟨110⟩ direction about a vacant normal lattice site; I_3 [⟨111⟩ split interstitial, or crowdion, Fig. 3(c)], two atoms are symmetrically split in a ⟨111⟩ direction about a vacant normal lattice site; I_4 [activated crowdion, Fig. 3(d)], an atom is located at the midpoint between two normal nearest-neighbor lattice sites; I_5 [octahedral interstitial, Fig. 3(e)], an atom is located at the midpoint between two normal second nearest-neighbor lattice sites; and I_6 [tetrahedral interstitial, Fig. 3(f)], an atom is located at the midpoint between two nearest octahedral interstitial sites.

[14] H. B. Huntington, in *Solid State Physics*, edited by F. Seitz and D. Turnbull (Academic Press Inc., New York, 1958), Vol. 7.

In the three "split" cases the pairs of atoms are approximately 1.5 a_0 apart (a_0=half-lattice constant).

Configuration I_2, the ⟨110⟩ split interstitial, is the minimum energy configuration and is, therefore, stable, in agreement with the results of Erginsoy *et al.*,[7] while I_3, the ⟨111⟩ split interstitial, is just barely a local minimum, i.e., metastable. The energy and volume expansion for the various interstitial configurations are given in Table III. I_7 is the saddle-point configuration for motion of the interstitial, and is somewhat awkward to describe because it does not have much symmetry. If the initial configuration is a [110] split interstitial centered at (0,0,0), the next equilibrium configuration after one jump might be a [101] split interstitial centered at (1,1,1) a_0. The saddle point for this step is at (0.50, 0.69, 0.31) a_0. The migration sequence $I_2 \rightarrow I_7 \rightarrow I_2$ is shown in Fig. 4., and the activation energy for this process was found to be 0.33 eV. The calculation also gave an activation volume for motion of 0.1 atomic volume.

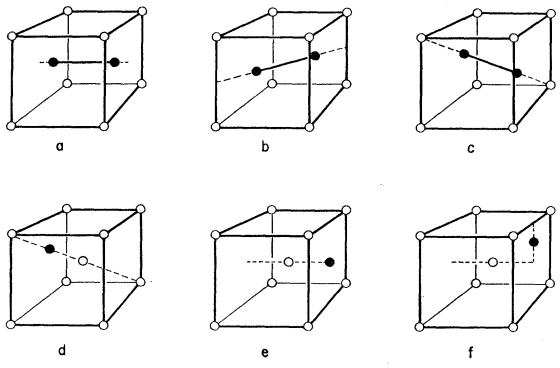

FIG. 3. Six iron interstitial configurations: (a) I_1 or ⟨100⟩ split interstitial; (b) I_2 or ⟨110⟩ split interstitials; (c) I_3, ⟨111⟩ split interstitial or crowdion; (d) I_4 or activated crowdion; (e) I_5 or octahedral interstitial; and (f) I_6 or tetrahedral interstitial.

The crowdion configuration I_3 is metastable, but by less than 0.01 eV, and the crowdion migration sequence $I_3 \rightarrow I_4 \rightarrow I_3$ has an activation energy for motion of 0.04 eV. The activation energy for rotation of a split interstitial, holding the center fixed, was found to be 0.33 eV, the same as the motion energy.

In order to make a complete study of interstitials it was necessary to check for the possible existence of other equilibrium configurations. In a manner similar to that used for copper[2] it was found to be possible to define a configuration by three coordinates. The iron calculations show that no two atoms ever approach each other closer than 1.5 a_0, and that there is always one atom within a radius of 0.75 a_0 from each normal lattice site. Thus, there is always one atom outside a bcc lattice of spheres of radius 0.75 a_0, which atom is defined as the interstitial. If the remaining atoms are at equilibrium positions consistent with the interstitial position, the crystal energy may be considered as a function of just the interstitial coordinates. If two atoms are on opposite ends of a sphere diameter, each is considered half in and half out of the sphere. These are the "split" configurations, and if one atom of a split pair enters the sphere, the other moves away from the sphere and becomes the interstitial. The volume available to the interstitial that must be studied is greatly reduced by symmetry. The volume in which the interstitial coordinates have no symmetrically equivalent position is 1/48 atomic volume, and only about half of this volume is outside the spheres, so, in effect, only about 0.01 atomic volumes must be investigated.

TABLE III. Interstitial configurations (Ω=atomic volume).

Configuration	Energy above I_2(eV)	$\Delta V(\Omega)$
I_1	1.29	1.7
I_2	...	1.6
I_3	0.32	1.7
I_4	0.36	1.7
I_5	1.12	1.4
I_6	0.85	1.5
I_7	0.33	1.7

No further equilibrium configurations of interest were found. The general pattern of the interstitial energy contours was as follows: low energy pockets at I_2 sites; a plateau region containing I_3, I_4, and I_7; and high energies elsewhere. The plateau region is roughly an oblate spheroid with its axis along the line joining two nearest neighbors. It is centered at an I_4 site, has two I_3 sites on its surface where the axis pierces the surface and has six I_7 sites on its outer rim. Not only are the configurations within this region at about the same energy, but there are no steep contours between them.

Di-Interstitials

There are many possible di-interstitial configurations and the calculations showed that many of them are metastable. Di-interstitial configurations consist of two split-single interstitials in reasonably close proximity to each other: No cases were found which resulted in more complex configurations. The most stable di-interstitial is shown in Fig. 5(a), and has two split interstitials parallel to each other at nearest-neighbor lattice sites, with their axes perpendicular to the line

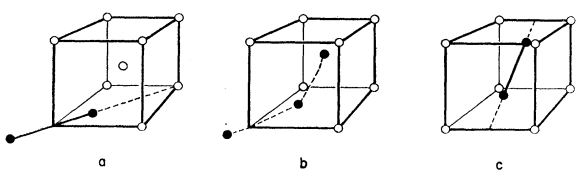

FIG. 4. The iron interstitial migration process. Configurations (a) and (c) are both I_2 configurations, and (b) is I_7, the saddle point configuration.

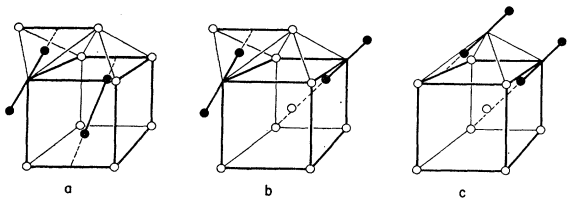

FIG. 5. The iron di-interstitial migration process. Configurations (a) and (c) are both stable di-interstitial configurations, and (b) is the intermediate step between (a) and (c).

joining their centers. The binding energy for this configuration relative to two separated interstitials was 1.08 eV and the associated volume relaxation was 0.3 atomic volumes.

The migration of di-interstitials is by a stepping process in which the two split interstitials partially dissociate. If the initial di-interstitial configuration is an interstitial split in the [110] direction at (0,0,0) a_0 and an interstitial split in the [110] direction at $(1,\bar{1},1)$ a_0, the intermediate configuration might be an interstitial split in the [110] direction at (0,0,0) a_0 and an interstitial split in the [011] direction at (2,0,2) a_0, and the final configuration would then be an interstitial split in the [011] direction at (1,1,1) a_0 and an interstitial split in the [011] direction at (2,0,2) a_0. This two step process is shown in Fig. 5, and it should be noted that the interstitial moving in each step follows a single interstitial migration path. The di-interstitial motion energy was 0.18 eV and the activation volume for motion was 0.3 atomic volumes.

The separation distance at which two split interstitials are bound as a di-interstitial did not have a well defined cutoff, but was calculated to be about 4.4 a_0. This is an average since the value depends upon the direction between the interstitials as well as their individual orientations. This range corresponds to a region of roughly 88 atomic volumes in which split interstitials have positive binding energy.

Vacancies and Di-Vacancies

The vacancy problem was straightforward compared to the interstitial calculations. The stable vacancy was the configuration in which an atom was missing from a normal lattice site, and the migration process consisted of a nearest-neighbor atom to the vacancy jumping from its normal lattice site to the vacancy site, thus filling in the vacancy and leaving a new vacancy behind. This process may also be thought of as the vacancy migrating by jumping to a nearest-neighboring lattice site. The migration energy was found to be 0.68 eV and the activation volume for motion was negligible.

The potential barrier for vacancy motion had a slight depression at the midpoint, i.e., the symmetric configuration at the midpoint of the process was not the saddle point but a local minimum. A single migration jump, therefore, had two saddle points as is shown in Fig. 6, where the energy of the configuration is plotted as a function of the position of the migrating atom. The existence of this metastable configuration should have little physical significance, however, since it is metastable by only about 0.04 eV.

A di-vacancy consists of two single vacancies in close proximity to each other. The most stable di-vacancy was that in which two vacancies were at second nearest-neighboring lattice sites, and the binding energy was 0.20 eV. The binding volume, or volume decrease of the lattice upon formation of a di-vacancy, was 0.1 atomic volumes. Vacancies at nearest neighboring sites were bound by 0.13 eV and vacancies at fourth nearest-neighboring sites were bound by 0.05 eV. No other pairs had an appreciable binding energy.

Di-vacancy migration was by a stepping process, in each step of which one of the vacancies of a di-vacancy pair moved as a single vacancy. Two possible migration processes were important; where the configuration changes from second nearest neighbor to nearest neighbor and back to second nearest neighbor, and from second to third and back to second nearest neighbor. The energy barrier for half of each of these migration paths is shown in Fig. 7, where the solid line is the energy barrier for migration via the third nearest-neighbor configuration and the dashed line is the energy barrier for migration via the nearest-neighbor configuration. The motion energies are 0.66 and 0.78 eV, respectively, and the activation volumes are negligible. These curves are seen to bear a strong resemblance to the curve in Fig. 6, so that a divacancy step may be thought of as a perturbed single vacancy step.

Motion by the third nearest neighbor mechanism always leaves the orientation of the divacancy un-

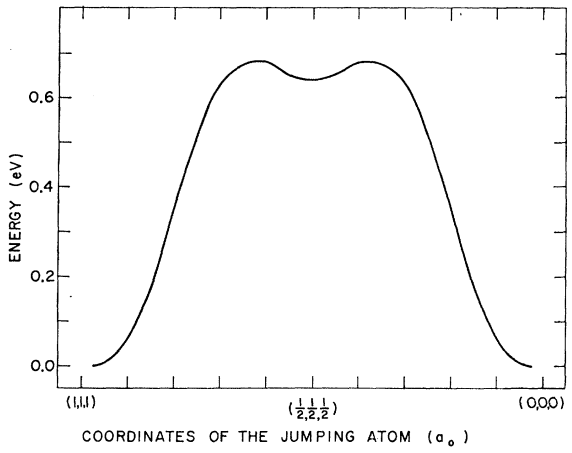

FIG. 6. The vacancy migration energy barrier. The energy of the configuration is shown as a function of the position of the jumping atom, as the vacancy migrates from (0,0,0) at the left to (1,1,1) at the right. The curve does not extend to (1,1,1) and (0,0,0) because the atom relaxes towards the vacancy.

altered, while the orientation may be changed by a nearest neighbor process. The nearest-neighbor configuration also may act as a trap, since 0.71 eV are required for the nearest neighbor to second nearest-neighbor divacancy transition.

A summary of these results is given in Table IV. Interstitial motion is not by the same mechanism as interstitial reorientation, although the energy and volume are the same. The corresponding di-interstitial processes are the same. Vacancies have the symmetry of the lattice and therefore do not have any reorientation process associated with them.

TABLE IV. Summary of results (energy in eV, volume in atomic volumes).

	Motion energy	Motion volume	Binding energy	Binding volume
Interstitial	0.33	0.1		
Crowdion	0.04	0.0		
Di-interstitial	0.18	0.3	1.08	0.3
Vacancy	0.68	0.0		
Di-interstitial	0.66	0.0	0.20	0.1
Interstitial	0.33	0.1	Reorientation	
Di-interstitial	0.18	0.3		
Divacancy	0.78	0.0		

DISCUSSION

Results

Very little experimental data are available pertaining to the results reported in the present paper, but some comparisons may be made for interstitial migration. Lucasson and Walker[8] have obtained isochronal resistivity annealing curves for iron and copper after irradiation with electrons at energies slightly above threshold. They also found that the stage I iron and copper annealing curves can be superposed if the iron temperature scale is reduced by a factor of 2.5.[15] Corbett, Smith, and Walker[16] have found an energy value of 0.12 eV for annealing of stages I_d and I_e in copper and have ascribed this annealing to interstitial migration. Assuming that the corresponding annealing stages in iron are also due to interstitial migration, and assuming that the pre-exponential factor associated with the migration processes of the iron and copper interstitials are roughly the same, then the iron interstitial migration energy is 0.30 eV. The calculated value was 0.33 eV, in very good agreement.

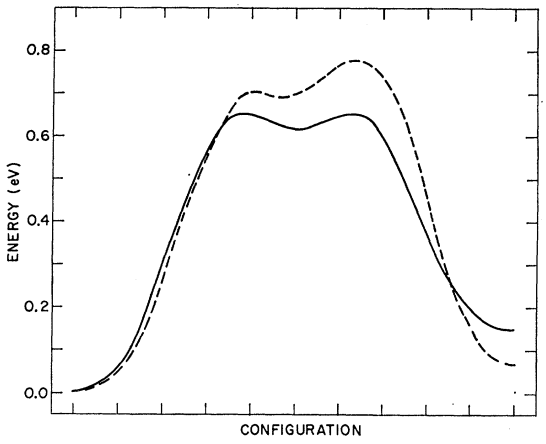

FIG. 7. The divacancy migration energy barrier. The energy of the configuration is plotted as a function of a configuration coordinate (similar to the coordinate of the jumping atom) as the divacancy transforms from a second nearest neighbor configuration on the left to a third nearest neighbor configuration along the solid line and a first nearest-neighbor configuration along the dashed line. Both curves have a mirror image repeat to the right of the drawn curves by which the migration process is completed.

In an internal fraction experiment by Wagenblast and Damask,[17] which searched for a relaxation associated with the interstitial in irradiated iron, the irradiation was performed at 140°K and the relaxation was looked for at higher temperatures, with negative results. Using the interpretation that interstitials anneal in stage I, the work of Lucasson and Walker just discussed shows that the iron interstitial anneals out of iron in ten minutes at 120°K. Thus, this interpretation is consistent with the Wagenblast and Damask findings.

Another interpretation of annealing in copper is that crowdions migrate in stages I_d and I_e and interstitials migrate in stage III.[18] The present calculations of crowdion stability and motion energy do not support this interpretation for iron. The Wagenblast and Damask experiment also does not support this interpretation since they found no indication of an oriented defect over a wide temperature range (140° to 385°K) in iron.

No direct experimental evidence is available for the motion energy of vacancies in iron. The activation energy for self-diffusion in α iron is 2.6 eV,[19] which is the sum of formation and motion energies. Theoretical estimates by Brooks[20] and by Mehl, Swanson, and Pound[21] indicate that the vacancy formation energy is considerably larger than the vacancy motion energy for bcc crystals, so that the motion energy of 0.68 eV reported in the present paper is not unreasonable compared to the self-diffusion energy. However, Damask

[15] P. G. Lucasson and R. M. Walker, Phys. Rev. **127**, 1130 (1962).
[16] J. W. Corbett, R. B. Smith, and R. M. Walker, Phys. Rev. **114**, 1460 (1959).
[17] H. Wagenblast and A. C. Damask, Acta Met. **10**, 333 (1962).
[18] C. J. Meechan, A. Sosin, and J. A. Brinkman, Phys. Rev. **120**, 411 (1960). A. Seeger, in *Proceedings of the Symposium on Radiation Damage in Solids* (International Atomic Energy Agency, Vienna, 1962), Vol. 1, p. 101.
[19] F. S. Buffington, I. D. Bakalar, and M. Cohen, J. Metals **4**, 859 (1952).
[20] H. Brooks, in *Impurities and Imperfections* (American Society for Metals, Cleveland, 1955), p. 1.
[21] R. F. Mehl, M. Swanson, and G. M. Pound, Acta Met. **9**, 256 (1961).

et al.,[22] in an extensive study of carbon in α iron did not find a vacancy annealing stage at temperatures which would correspond to a motion energy of 0.68 eV, and the model which they proposed to explain their results assumes that vacancies move at a temperature corresponding to a motion energy of greater than about 1.0 eV.

The present results indicate that none of the defects studied are amenable to internal friction studies. Vacancies have the symmetry of the lattice and are, therefore, eliminated from consideration. The energy to reorient di-vacancies is greater than their motion energy, and so they will anneal before being able to reorient. Both interstitials and di-interstitials require the same energy to migrate as to reorient (migration and reorientation are the same process for di-interstitials), and thus, internal friction experiments would be very difficult to perform as the concentration of defects would be decreasing at a temperature where internal friction would be large. This does not take into account the possibility that the relaxation strength associated with these defects might be sufficiently small so that internal friction could not be measured at experimentally obtainable concentrations. A detailed calculation of this effect was made for copper[23] for an oriented interstitial with the result that even if the defect were present in heavy concentrations, it would be very difficult to detect by internal friction.

Model

The results of the present calculations are considered to accurately represent the model: Increasing the size of the region in which the atoms are allowed full freedom to relax, using greater precision within the calculation, using a different relaxation scheme, etc., would not sensibly affect the results. The important question is whether or not the model satisfactorily represents the real crystal so that the results are meaningful.

This model completely neglects any contribution from the so-called electron redistribution energy, i.e., it does not account for the drastic alteration of the electron wave functions near the defect. The author knows of no method currently available to obtain any sensible estimate of how this term enters into the differences in energy between various configurations. It is felt, however, that in all probability the calculated vacancy migration energy would be increased. It is also felt that the configurations are determined primarily by the close repulsions, so that the electron redistribution would have very little affect upon the configurations.

The energy in this model is not a sensitive function of the volume, and thus, the volume changes for the various configurations should only be considered as a rough approximation.

The choice of a potential is a critical part of any calculation, and it is felt that the potential used in the present calculation is as good an approximation as may be made. It matches the experimental elastic moduli and is fitted to a number of other not unreasonable criteria. A major objection might be that it is cut off after the second nearest neighbor. Aside from the fact that increasing the range of the potential would greatly increase the complexity of the calculation, it is desirable to test the simplest reasonable model first and only incorporate more complex features where necessary. The assumption in using a short range potential is that longer range effects average out to give rise to the volume-dependent binding.

ACKNOWLEDGMENTS

The author wishes to thank Dr. C. Erginsoy, Dr. A. C. Damask, Dr. G. J. Dienes, and Dr. G. H. Vineyard for many discussions and suggestions during the course of this work.

[22] H. Wagenblast and A. C. Damask, Phys. Chem. Solids **23**, 22 (1962). F. E. Fujita and A. C. Damask, Acta Met. **12**, 331 (1964). R. A. Arndt and A. C. Damask, Acta Met. **12**, 341 (1964). H. Wagenblast, F. E. Fujita, and A. C. Damask, Acta Met. **12**, 347 (1964).

[23] H. B. Huntington and R. A. Johnson, Acta Met. **10**, 281 (1962).